Critical dynamics of an asymmetrically bidirectionally pumped optical microresonator

Jonathan M. Silver[1,*] Kenneth T. V. Grattan,[2] and Pascal Del'Haye[3,4,†]
[1]*National Physical Laboratory, Hampton Road, Teddington TW11 0LW, United Kingdom*
[2]*City, University of London, Northampton Square, London EC1V 0HB, United Kingdom*
[3]*Max Planck Institute for the Science of Light, Staudtstrasse 2, 91058 Erlangen, Germany*
[4]*Department of Physics, Friedrich-Alexander University Erlangen-Nuremberg, 91058 Erlangen, Germany*

(Received 23 March 2021; accepted 27 April 2021; published 12 October 2021)

An optical ring resonator with third-order, or Kerr, nonlinearity will exhibit symmetry breaking between the two counterpropagating circulating powers when pumped with sufficient power in both the clockwise and counterclockwise directions. This is due to the effects of self- and cross-phase modulation on the resonance frequencies in the two directions. The critical point of this symmetry breaking exhibits universal behaviors including divergent responsivity to external perturbations, critical slowing down, and scaling invariance. Here we derive a model for the critical dynamics of this system, first for a symmetrically pumped resonator and then for the general case of asymmetric pumping conditions and self- and cross-phase modulation coefficients. This theory not only provides a detailed understanding of the dynamical response of critical-point-enhanced optical gyroscopes and near-field sensors, but is also applicable to nonlinear critical points in a wide range of systems.

DOI: 10.1103/PhysRevA.104.043511

I. INTRODUCTION

Spontaneous symmetry breaking is ubiquitous in physics, occurring at every possible energy scale all the way from the Higgs mechanism [1] down to superconductivity [2], superfluidity [3], and other exotic quantum states of matter at ultracold temperatures [4]. Associated with every spontaneous symmetry-breaking transition is a critical point [5]. This is a point in parameter space on the boundary of the symmetry-broken regime where the symmetric state of the system is neither stable nor unstable, and which exhibits certain universal features. Firstly, the system will have divergent responsivity to external perturbations that break the symmetry of the system, exhibiting large excursions in response to tiny perturbations but always eventually returning to the symmetric state if the perturbation is removed. Secondly, the characteristic timescales and length scales (where relevant) of the system's response diverge: the system exhibits fluctuations at all length scales that decay with time according to a power law rather than exponentially and thus take exponentially longer to reach the steady state. This is often referred to as critical slowing down [5]. Thirdly, the equations of the system around the critical point exhibit scaling invariance, meaning that they are unchanged when the offsets of the various parameters from the critical point, as well as length and time, are scaled by certain powers of each other.

One system that exhibits spontaneous symmetry breaking of the discrete group C_2 (the cyclic group of order 2) is that of a symmetrically bidirectionally pumped optical microresonator with Kerr nonlinearity, in which the counterpropagating circulating powers will spontaneously deviate from each other [6–9]. This is an example of what is known as a pitchfork bifurcation due to the way in which one stable solution splits into two. This effect gives rise to a range of interesting and useful behaviors, including optical nonreciprocity [9], logic gates [10], memories [11], and self-switching [12]. Since it is clockwise-counterclockwise symmetry that is being broken, at a critical point the system exhibits divergent responsivity to perturbations that distinguish between the two directions, including most notably pump power and detuning differences. Since pump detuning differences can be induced via the Sagnac effect by rotating the entire setup, which causes the counterpropagating resonance frequencies to differ by an amount proportional to the rotation velocity [13], this critical point can be used to create a simple yet extremely sensitive gyroscope [14–16]. The Sagnac effect is related to but distinct from Fizeau drag, which was recently demonstrated in a similar experiment in which the microresonator was rotated but the rest of the setup remained stationary [17].

Critical-point-enhanced gyroscopes and other sensors such as those for refractive index changes [18,19] may be compared to ones that achieve divergent responsivities using exceptional points [20,21]. Although there has been significant interest in these recently, there is growing consensus that while exceptional points enhance responsivity they do not actually enhance sensitivity as noise is amplified by the same amount as the signal [22–24]. The same is true for critical-point-enhanced sensors, which unlike exceptional-point-based ones are also sensitive to pump power noise due to their reliance upon optical nonlinearity. We show explicitly in this paper that the responsivities to pump detuning and power differences are enhanced by the same factor. Nevertheless, the responsivity enhancement provides a simple means to increase sensitivity

*jonathan.silver@npl.co.uk
†pascal.delhaye@mpl.mpg.de

 ©2021 American Physical Society

by bypassing the noise floor of downstream components such as photodiodes, as long as the pump power and detuning noise sources can be sufficiently suppressed.

The development of critical-point-enhanced sensors requires a detailed understanding of the critical dynamics of the system, including its response to time-dependent and finite-amplitude inputs. In this paper we show that, in the limit as we approach the critical point, the dynamics are governed by a simple equation, from which the divergent responsivity, critical slowing down, and scaling invariance are manifestly apparent. This is done first in Sec. II for the simplest case of a symmetrically pumped resonator with a Kerr cross-phase modulation (XPM) coefficient twice as large as that of self-phase modulation (SPM), as is the case in any dielectric solid [25]. In Sec. III we show that the same critical point and behavior can occur even when the system itself is not symmetric, but when two different asymmetries, for example in pump power and detuning, balance each other [26]. We derive the exact condition for the critical point, as well as the equation for the critical dynamics, in an asymetrically pumped resonator with arbitrary and even asymmetric SPM and XPM coefficients.

The theory presented here applies not only to Kerr-related symmetry breaking between counterpropagating light, but also between different frequencies, propagation angles [27], and opposite circular polarizations [28–32], all of which obey the same equations. For instance, the asymmetric critical point was recently demonstrated for the polarization case in a fiber loop cavity [26]. Furthermore, this theory applies to systems where the Kerr effect is substituted with a Kerr-like interaction such as the magnetic nonlinearity [33], or even to similar nonlinear systems outside the optical domain altogether.

The ratio between the XPM and SPM coefficients can take different values in different materials, including less than 2 in semiconductors and gases due to diffusive effects, and as much as 7 for interaction between opposite circular polarizations in Kerr liquids [25,34]. Differences between the two mode volumes will lead to asymmetries in both the SPM and XPM coefficients, while asymmetric effective SPM coefficients but symmetric XPM coefficients can arise if the light in one of the modes is not monochromatic [16].

Finally, a condition is derived for decoupling the critical dynamics from the thermal nonlinearity [35], which, although perfectly symmetric in its action, is typically much larger than the Kerr effect, and could thus disrupt the critical dynamics in the case of asymmetric pumping conditions or SPM or XPM coefficients.

II. SYMMETRIC PUMPING CONDITIONS

When an optical ring resonator with Kerr, or $\chi^{(3)}$, nonlinearity is pumped with light of equal power and frequency in both directions, a spontaneous splitting can occur between the two counterpropagating circulating powers and resonance frequencies [6–8]. This occurs due to the interplay between the circulating-power-dependent Kerr shifts of the counterpropagating resonance frequencies and the detuning-dependent circulating powers due to the pump frequency being on the side of the resonance. The Kerr effect decreases each resonance frequency by an amount proportional to the circulating power in that mode (from SPM) plus twice that in the counterpropagating mode (from XPM). This means that the resonance frequency is lower in the direction with less circulating power. If the pump is blue-detuned from the resonance—a necessary condition for passive thermal [35] and Kerr locking of the resonance to the pump frequency—then the direction with less circulating power will be shifted further from the pump, which in turn increases the circulating power difference, creating positive feedback that causes the symmetry to spontaneously break.

TABLE I. Dimensionless quantities used in this paper. η_{in} is the resonant in-coupling efficiency equal to $4\kappa\gamma_0/\gamma^2$ where κ, γ_0, and $\gamma = \gamma_0 + \kappa$ are the coupling, intrinsic and total half-linewidths respectively. $P_{\text{in},1,2}$ and $P_{\text{circ},1,2}$ are the pump and circulating powers respectively. $P_0 = \pi n_0^2 V/(n_2 \lambda Q Q_0)$ is the characteristic in-coupled power required for Kerr nonlinear effects, where n_0 and n_2 are the linear and nonlinear refractive indices, V is the mode volume, and $Q = \omega_0/(2\gamma)$ and $Q_0 = \omega_0/(2\gamma_0)$ are the loaded and intrinsic quality factors respectively for cavity resonance frequency ω_0 (without Kerr shift). $\mathcal{F}_0 = \Delta\omega_{\text{FSR}}/(2\gamma_0)$ is the cavity's intrinsic finesse for free spectral range $\Delta\omega_{\text{FSR}}$, and $\omega_{1,2}$ are the pump frequencies.

Symbol	Description	Formula
$\tilde{p}_{1,2}$	Pump powers	$\eta_{\text{in}} P_{\text{in},1,2}/P_0$
$p_{1,2}$	Circulating powers	$2\pi P_{\text{circ},1,2}/(\mathcal{F}_0 P_0)$
$\Delta_{1,2}$	Pump detunings from resonance frequency without Kerr shift	$(\omega_0 - \omega_{1,2})/\gamma$
$\tilde{e}_{1,2}$	Pump field amplitudes	$\tilde{p}_{1,2} = \lvert\tilde{e}_{1,2}\rvert^2$
$e_{1,2}$	Circulating field amplitudes	$p_{1,2} = \lvert e_{1,2}\rvert^2$

This effect may be described by solving the following pair of simultaneous equations for the circulating powers $p_{1,2}$ in the two counterpropagating directions in terms of the pump powers $\tilde{p}_{1,2}$ and detunings $\Delta_{1,2}$ from the resonance without Kerr shift [8]:

$$p_{1,2} = \frac{\tilde{p}_{1,2}}{1 + (p_{1,2} + 2p_{2,1} - \Delta_{1,2})^2}. \tag{1}$$

Here, and throughout this paper, we use the dimensionless quantities defined in Table I. Equation (1) is simply the dimensionless form of the Lorentzian resonance curves for the circulating powers, taking into account the Kerr shifts. Note the factor of 2 in front of the counterpropagating circulating power, corresponding to the ratio between the strengths of XPM and SPM in a dielectric solid with Kerr nonlinearity; this ratio is generalized in Sec. III. Under the symmetrical pumping conditions $\tilde{p}_{1,2} = \tilde{p}$ and $\Delta_{1,2} = \Delta$, symmetry breaking occurs for a range of Δ if $\tilde{p}$ exceeds $8/(3\sqrt{3}) \simeq 1.54$ [6,8]. This is illustrated in Fig. 1 for $\tilde{p}$ a little above this threshold. As the detuning approaches the symmetry-broken regime, the difference between p_1 and p_2 exhibits increasing responsivity to perturbations that break the directional symmetry, such as pump power or detuning differences. This responsivity diverges at each of the critical points A_1 and A_2, at which the finite-amplitude response is proportional to the cube root of the perturbation.

We begin with the dimensionless equations for the time derivatives $\dot{e}_{1,2}$ of the electric field amplitudes $e_{1,2}$ in the

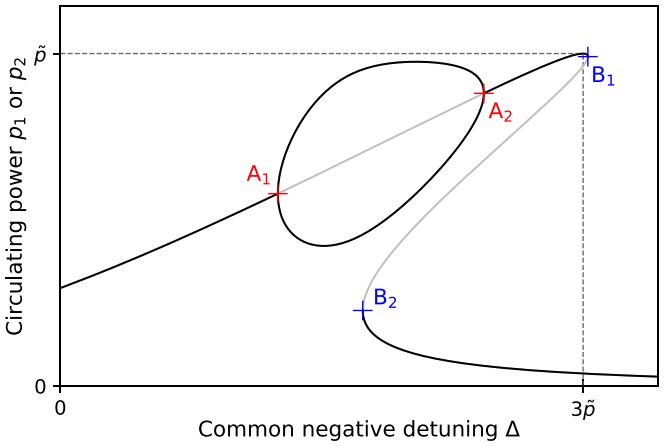

FIG. 1. Solutions to Eq. (1) under symmetric pumping conditions $\tilde{p}_{1,2} = \tilde{p}$ and $\Delta_{1,2} = \Delta$, illustrated for $\tilde{p} = 1.75$. Solid black and grey lines represent stable and unstable solutions respectively. Between the critical points A_1 and A_2, the symmetric solution $p_1 = p_2$ is unstable and two new symmetry-broken stable solutions appear in which p_1 and p_2 take the opposite branches shown. Another unstable region lies between B_1 and B_2, which occurs even for a unidirectionally pumped resonator and here corresponds to a symmetric bistability.

two counterpropagating modes in the rotating frames of their respective pump fields [8], which yield Eq. (1) in the steady state:

$$\dot{e}_{1,2} = \tilde{e}_{1,2} - [1 + i(|e_{1,2}|^2 + 2|e_{2,1}|^2 - \Delta_{1,2})]e_{1,2}. \quad (2)$$

Once again, the notation is given in Table I, and time is in units of $1/\gamma$. A rigorous derivation of Eq. (2) from first principles is given in [36]. We shall assume for now that $\tilde{e}_1 = \tilde{e}_2 = \tilde{e}$ is constant with time, while $\Delta_{1,2}$ undergo small time-dependent perturbations around a common value Δ, with $\tilde{e}$ and Δ chosen so as to place the system at a critical point. We are interested in the perturbative dynamics of $e_{1,2}$ around a symmetric steady-state solution $e_{1,2} = e$ that satisfies $\tilde{e} = [1 + i(3p - \Delta)]e$, where the circulating power in each direction $p = |e|^2$.

Figure 2 shows the exact response of such a system to a sinusoidal detuning perturbation $\delta_d(t)$ that is purely differential mode, i.e., equal and opposite, between the two directions. Such a perturbation could be induced for example by a rotation of the resonator. The response takes the form of a differential-mode perturbation to the circulating powers, namely $p_d(t) = (p_1 - p_2)/2$, a quantity that is easy to measure experimentally. It is explicitly shown that close to the critical point, the response becomes invariant to the scaling transformation represented by varying the parameter κ while maintaining $p_d \propto \kappa$, $\delta_d(t) \propto \kappa^3$, and $t \propto \kappa^{-2}$, where taking $\kappa \to 0$ represents zooming into the critical point. The critical behaviors of divergent steady-state responsivity and critical slowing down can be seen from the facts that $p_d/\delta_d \propto \kappa^{-2}$ and $t \propto \kappa^{-2}$ respectively. All this suggests that in the limit close to the critical point, the dynamics of the system can be described by a simple effective theory that is invariant under this particular scaling transformation. The rest of this paper is concerned with rigorously deriving such a theory, which

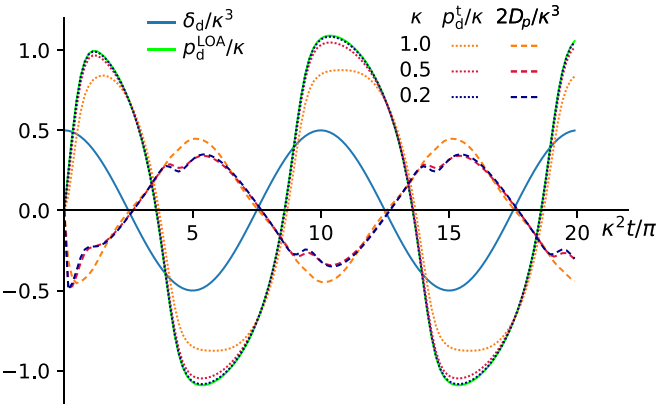

FIG. 2. Response of a resonator to a sinusoidally modulated splitting between clockwise and counterclockwise modes (e.g., from a sinusoidal back-and-forth rotation of the resonator). The response is scale invariant close to the critical point. Starting from the steady state at the symmetric critical point $p = 1$, $\Delta = 2$, a sinusoidal, purely differential-mode detuning perturbation of the form $\Delta_1(t) = \Delta + \delta_d(t)$, $\Delta_2(t) = \Delta - \delta_d(t)$, with $\delta_d(t) = \delta_d^{AC} \cos \omega t$, is applied from time $t = 0$. This is done using $\delta_d^{AC} = 0.5\kappa^3$ and $\omega = 0.2\kappa^2$ for three values of the scaling parameter κ, namely 1.0, 0.5, and 0.2. The solid blue line shows $\delta_d(t)/\kappa^3$ vs $\kappa^2 t/\pi$, which is the same curve in each case. The dotted lines show the resulting "true" differential-mode circulating powers $p_d^t = (p_1 - p_2)/2$ calculated directly using Eq. (2), divided by κ, for each value of κ. As κ decreases, these converge on a single curve, suggesting that close to the critical point the system's dynamics can be described by effective equations that are scale-invariant with respect to κ. The solid green line correspondingly shows p_d/κ calculated using the scale-invariant leading-order approximation ("LOA") developed in this paper, which is the limit of the true curves. The dashed lines show the differences between the true and LOA solutions, $D_p = p_d^t - p_d^{LOA}$, plotted as $2D_p/\kappa^3$. The fact that these also converge to a single curve demonstrates that the fractional error in the leading-order approximation scales as κ^2.

indeed is shown in Fig. 2 to match the exact theory in the limit $\kappa \to 0$.

Choosing the phase of $\tilde{e}$ such that e is real and positive, we let

$$\Delta_{1,2} = \Delta + \delta_{1,2},$$
$$e_{1,2} = e + f_{1,2} + ig_{1,2}, \quad (3)$$

where $\delta_{1,2}$, $f_{1,2}$, and $g_{1,2}$ are all real, and represent perturbations to the pump detunings and circulating field amplitudes and phases respectively. Substituting these into Eq. (2), we can express the dynamical equations of $f_{1,2}$ and $g_{1,2}$ in the form

$$\dot{\mathbf{f}} = \mathbf{M}\mathbf{f} + \mathbf{d} + \mathbf{D}\mathbf{f} + \mathbf{k} + \mathbf{l}, \quad (4)$$

where

$$\mathbf{f} = \begin{pmatrix} f_1 \\ g_1 \\ f_2 \\ g_2 \end{pmatrix}, \quad \mathbf{d} = e\begin{pmatrix} 0 \\ \delta_1 \\ 0 \\ \delta_2 \end{pmatrix}, \quad \mathbf{D} = \begin{pmatrix} 0 & -\delta_1 & 0 & 0 \\ \delta_1 & 0 & 0 & 0 \\ 0 & 0 & 0 & -\delta_2 \\ 0 & 0 & \delta_2 & 0 \end{pmatrix},$$

$$\mathbf{M} = \begin{pmatrix} -1 & 3p - \Delta & 0 & 0 \\ \Delta - 5p & -1 & -4p & 0 \\ 0 & 0 & -1 & 3p - \Delta \\ -4p & 0 & \Delta - 5p & -1 \end{pmatrix},$$

$$\mathbf{k} = e\begin{pmatrix} g_1(2f_1+4f_2) \\ -\left(3f_1^2+g_1^2+2f_2^2+2g_2^2+4f_1f_2\right) \\ g_2(2f_2+4f_1) \\ -\left(3f_2^2+g_2^2+2f_1^2+2g_1^2+4f_1f_2\right) \end{pmatrix},$$

$$\mathbf{l} = \begin{pmatrix} g_1\left(f_1^2+g_1^2+2f_2^2+2g_2^2\right) \\ -f_1\left(f_1^2+g_1^2+2f_2^2+2g_2^2\right) \\ g_2\left(f_2^2+g_2^2+2f_1^2+2g_1^2\right) \\ -f_2\left(f_2^2+g_2^2+2f_1^2+2g_1^2\right) \end{pmatrix}. \tag{5}$$

We begin by considering the linear response of the system around the steady-state solution, which is governed by $\dot{\mathbf{f}} = \mathbf{M}\mathbf{f} + \mathbf{d}$. Here we have kept only the terms that are first-order in the perturbations f_i, g_i, and δ_i, discarding those that are second or third order. Inspecting the eigenvalues of $\mathbf{M}$, we find that the steady-state solution is unstable when one of the following two conditions is satisfied, as each condition causes a different eigenvalue to be real and positive:

$$(p-\Delta)(3p-\Delta) < -1, \tag{6}$$

$$(3p-\Delta)(9p-\Delta) < -1. \tag{7}$$

Since $p > 0$, Eq. (6) can hold only when $3p-\Delta > 0$, and (7) only when $3p-\Delta < 0$. Since $3p-\Delta$ is the laser detuning from the Kerr-shifted resonance, this means that (6) must correspond to the symmetry-broken region between the critical points A_1 and A_2 in Fig. 1, and (7) to the region between B_1 and B_2. The critical points are thus characterized by the boundary of (6):

$$(p-\Delta)(3p-\Delta) = -1. \tag{8}$$

Under this condition, which shall be assumed to hold for the rest of this section, the eigenvectors $\mathbf{v}_i$ and corresponding eigenvalues λ_i of $\mathbf{M}$ are

$$\mathbf{v}_1 = \begin{pmatrix} -a \\ -1 \\ a \\ 1 \end{pmatrix}, \quad \lambda_1 = 0; \quad \mathbf{v}_2 = \begin{pmatrix} a \\ -1 \\ -a \\ 1 \end{pmatrix}, \quad \lambda_2 = -2;$$

$$\mathbf{v}_3 = \begin{pmatrix} -ir \\ 1 \\ -ir \\ 1 \end{pmatrix}, \quad \lambda_3 = -1 + ia/r;$$

$$\mathbf{v}_4 = \begin{pmatrix} ir \\ 1 \\ ir \\ 1 \end{pmatrix}, \quad \lambda_4 = -1 - ia/r, \tag{9}$$

where $a = 3p-\Delta$ and $r = \sqrt{(3p-\Delta)/(9p-\Delta)}$ are real and positive. The slow critical dynamics will thus be dominated by $\mathbf{v}_1$ as this has a zero eigenvalue, whereas the other three have eigenvalues with negative real parts of order unity, and thus decay away on a timescale of the order of the cavity lifetime. Note that $\mathbf{v}_1$ corresponds to an antisymmetric combined amplitude and phase perturbation.

Turning again to Eq. (4) including all its nonlinear terms, we will now express it in this eigenbasis by using the inverse basis $\{\mathbf{u}_i\} : \mathbf{u}_i \cdot \mathbf{v}_j = \delta_{ij}$, where δ_{ij} is the Kronecker delta, to decompose

$$\mathbf{f} = \sum_i \mu_i \mathbf{v}_i, \quad \mathbf{d} = \sum_i d_i \mathbf{v}_i,$$

$$\mathbf{D} = \sum_{i,j} D_{ij}\mathbf{v}_i\mathbf{u}_j^{\mathrm{T}}, \quad \mathbf{k} = \sum_{i,j,k} K_{ijk}\mathbf{v}_i\mu_j\mu_k,$$

$$\text{and} \quad \mathbf{l} = \sum_{i,j,k,l} L_{ijkl}\mathbf{v}_i\mu_j\mu_k\mu_l, \tag{10}$$

where i, j, k, l index the eigenvectors and hence run from 1 to 4, and μ_i is the projection of $\mathbf{f}$ along $\mathbf{v}_i$:

$$\dot{\mu}_i = \lambda_i\mu_i + d_i + \sum_j D_{ij}\mu_j + \sum_{j,k} K_{ijk}\mu_j\mu_k + \sum_{j,k,l} L_{ijkl}\mu_j\mu_k\mu_l. \tag{11}$$

To extract the dynamics in the region immediately surrounding the critical point, we will start by removing the driving terms d_i and D_{ij}:

$$\dot{\mu}_i = \lambda_i\mu_i + \sum_{j,k} K_{ijk}\mu_j\mu_k + \sum_{j,k,l} L_{ijkl}\mu_j\mu_k\mu_l. \tag{12}$$

For small perturbations and responses around the critical point, we may say that $|\mu_1| \ll 1$. Furthermore, since μ_2, μ_3, and μ_4, unlike μ_1, have exponential decay times that are short compared to the timescale of the critical dynamics as discussed above, it is safe to assume that $|\mu_i| \ll |\mu_1|$, $i \neq 1$. Nevertheless, we shall see that these cannot be ignored entirely as they still contribute to the dynamics of μ_1. Looking at the case $i = 1$ in Eq. (12), since $\lambda_1 = 0$, the leading term in $\dot{\mu}_1$ would be $K_{111}\mu_1^2$. However, $K_{111} = 0$ by considerations of directional symmetry, i.e., switching the 1 and 2 directions. This leaves

$$\dot{\mu}_1 = 2\sum_{i\neq 1} K_{11i}\mu_1\mu_i + L_{1111}\mu_1^3 \tag{13}$$

to leading order, assuming that $K_{ijk} = K_{ikj}$ by construction. Looking again at Eq. (12), we can see that to leading order, the other μ_i obey the following quasi-steady-state equations:

$$0 = \lambda_i\mu_i + K_{i11}\mu_1^2, \quad i \neq 1. \tag{14}$$

Noting that also $K_{211} = 0$ by directional symmetry, this can be combined with Eq. (13) to give

$$\dot{\mu}_1 = \left(L_{1111} - 2\sum_{i=3,4}\frac{K_{11i}K_{i11}}{\lambda_i}\right)\mu_1^3. \tag{15}$$

Both terms are of equal order, so indeed we cannot neglect the effect of μ_3 and μ_4 on the dynamics of μ_1. Furthermore, we may observe that $\mu_{3,4}$ scale as μ_1^2 and $\dot{\mu}_1$ scales as μ_1^3, the latter confirming that the timescale of the dynamics increases (as μ_1^{-2}) as we zoom closer and closer into the critical point.

Equation (15) describes the free evolution of the system to leading order. Now we reintroduce the driving terms d_i and D_{ij} at magnitudes that preserve the above hierarchy of scalings. For this, it is useful to introduce the common- and differential-mode detunings $\delta_c = (\delta_1+\delta_2)/2$ and

$\delta_d = (\delta_1 - \delta_2)/2$, and to note that

$$d_1 = -\frac{e\delta_d}{2}, \quad d_{3,4} = \frac{e\delta_c}{2}, \quad D_{11} = (2p - \Delta)\delta_c. \tag{16}$$

Substituting the first two of these into Eq. (11) for the relevant i, we deduce that δ_d scales as μ_1^3 and δ_c as μ_1^2, and therefore that the only element of D_{ij} that can possibly affect the dynamics to leading order is D_{11}. This leaves us, to leading order, with

$$\mu_i = -\frac{K_{i11}\mu_1^2 + e\delta_c/2}{\lambda_i} \quad \text{for} \quad i = 3, 4, \tag{17}$$

satisfying $\mu_4 = \mu_3^*$ since $K_{114} = K_{113}^*$ and $\lambda_4 = \lambda_3^*$, and

$$\begin{aligned}\dot{\mu}_1 &= -\frac{e\delta_d}{2} + \left[(2p - \Delta) - e\left(\frac{K_{113}}{\lambda_3} + \frac{K_{114}}{\lambda_4}\right)\right]\delta_c\mu_1 \\ &\quad + \left[L_{1111} - 2\left(\frac{K_{113}K_{311}}{\lambda_3} + \frac{K_{114}K_{411}}{\lambda_4}\right)\right]\mu_1^3 \\ &= -\frac{e\delta_d}{2} + \frac{5p - 2\Delta}{4}\delta_c\mu_1 \\ &\quad + \frac{(3p - \Delta)(4 + 4p\Delta - 15p^2)}{2}\mu_1^3. \end{aligned} \tag{18}$$

So far, for conciseness, we have not considered the effect of pump power perturbations. It turns out that these have a very similar effect to detuning perturbations; their treatment is summarized as follows. We may represent small fractional pump power perturbations $\epsilon_{1,2}$ by letting $\tilde{e}_{1,2} = \tilde{e}(1 + \epsilon_{1,2}/2)$ and consequently adding $e(\epsilon_1, a\epsilon_1, \epsilon_2, a\epsilon_2)/2$ to $\mathbf{d}$. Decomposing these into common- and differential-mode components $\epsilon_c = (\epsilon_1 + \epsilon_2)/2$ and $\epsilon_d = (\epsilon_1 - \epsilon_2)/2$ and revisiting the above steps, we find that ϵ_d scales as μ_1^3 and ϵ_c as μ_1^2 just as with detuning perturbations, and that Eq. (18) becomes

$$\begin{aligned}\dot{\mu}_1 &= -\frac{e}{2}(\delta_d + p\epsilon_d) + \left(\frac{5p - 2\Delta}{4}\delta_c + \frac{2\Delta - 3p}{4}p\epsilon_c\right)\mu_1 \\ &\quad + \frac{(3p - \Delta)(4 + 4p\Delta - 15p^2)}{2}\mu_1^3. \end{aligned} \tag{19}$$

Interestingly, if we include pump *phase* perturbations, for example by allowing $\epsilon_{1,2}$ to be complex, we find that they (as distinct from detuning perturbations which are analogous to their time derivatives) play no role in the critical dynamics to leading order. This is actually expected, since Eq. (2) is invariant under static phase rotations of $\tilde{e}_{1,2}$, as long as the same rotations are applied respectively to $e_{1,2}$.

Importantly, the coefficient of μ_1^3 in Eqs. (18) and (19) is always negative, which can be seen by substituting in Eq. (8) to give $-(3p - \Delta)((2\Delta - 5p)^2 + 2p^2)/2$. We can therefore reexpress (19) in the form

$$\dot{y} = -y^3 + xy + z, \tag{20}$$

where

$$\begin{aligned} x &= \frac{5p - 2\Delta}{4}\delta_c + \frac{2\Delta - 3p}{4}p\epsilon_c, \\ y &= -\sqrt{\frac{(3p - \Delta)(15p^2 - 4p\Delta - 4)}{2}}\mu_1, \\ z &= \sqrt{\frac{p(3p - \Delta)(15p^2 - 4p\Delta - 4)}{8}}(\delta_d + p\epsilon_d). \end{aligned} \tag{21}$$

From the expression for $\mathbf{v}_1$ in Eq. (9) we can relate y to the observable differential-mode (normalized) coupled power $p_d = (p_1 - p_2)/2$ to leading order as follows:

$$p_d = e(f_1 - f_2) = \sqrt{\frac{8p(3p - \Delta)}{15p^2 - 4p\Delta - 4}}\, y. \tag{22}$$

As expected, Eq. (20) is invariant under the transformation in which x, y, z, and t (time) scale as κ^2, κ, κ^3, and κ^{-2} respectively for some parameter κ. Scaling invariances such as this are a universal feature of critical points in many areas of physics, such as ferromagnetism, superconductivity, and liquid-gas transitions [5]. Equations (20) to (22) were used to produce the curve of $p_d^{\mathrm{LOA}}/\kappa$ in Fig. 2, which is the limit of p_d^{t}/κ for $\kappa \to 0$.

The dynamics of y under Eq. (20) can be summarized as an interplay between three simple behaviors, each of which occurs in its pure form when two of the three terms containing y can be neglected. These behaviors are cube root ($y = z^{1/3}$), proportional ($y = -z/x$), and integrator ($\dot{y} = z$). Furthermore, Eq. (20) indicates the presence of two universal critical behaviors, namely divergent steady-state responsivity ($|y/z| \to \infty$ as $|x|, |y|, |\dot{y}| \to 0$) and critical slowing down ($|\dot{y}/y| \to 0$ as $|x|, |y|, |z| \to 0$). These critical behaviors are apparent in Fig. 2 from the fact that the ratio of the output p_d to the input δ_d, and the time lag between δ_d and p_d, both scale as $1/\kappa^2$ and hence diverge as $\kappa \to 0$.

III. ASYMMETRIC SPM AND XPM COEFFICIENTS AND PUMPING CONDITIONS

In this section we generalize the theory to asymmetric SPM and XPM coefficients and pump powers and detunings. This is based on an extension of Eq. (2) to general SPM and XPM coefficients A_{ij}:

$$\dot{e}_j = \tilde{e}_j - \left[1 + i\left(\sum_k A_{jk}|e_k|^2 - \Delta_j\right)\right]e_j, \tag{23}$$

which reproduces Eq. (2) for $A_{11} = A_{22} = 1$ and $A_{12} = A_{21} = 2$. This time, we expand this around a general asymmetric steady-state solution $\Delta_i = \Delta_i^0$, $e_i = e_i^0 \in \mathbb{R}^+$, $\tilde{e}_j = \tilde{e}_j^0 = (1 + ia_j)e_j^0$, where $a_i = \sum_j A_{ij}p_j^0 - \Delta_i^0$, $p_i^0 = e_i^{0\,2}$. For completeness, in addition to detuning perturbations δ_i, we include fractional pump power and pump phase perturbations, ϵ_i and ϕ_i respectively, from the start (although static phase perturbations ϕ_i will again be found to have no effect on the critical dynamics):

$$\begin{aligned} \Delta_i &= \Delta_i^0 + \delta_i, \\ \tilde{e}_j &= \tilde{e}_j^0\left(1 + \frac{\epsilon_j}{2} + i\phi_j\right), \\ e_j &= e_j^0 + f_j + ig_j. \end{aligned} \tag{24}$$

We still express the time evolution of f_i and g_i in the form given in Eq. (4), but with the following modifications:

$$\mathbf{d} = \begin{pmatrix} e_1^0\varepsilon_1 \\ e_1^0(\delta_1+\zeta_1) \\ e_2^0\varepsilon_2 \\ e_2^0(\delta_2+\zeta_2) \end{pmatrix}, \quad \mathbf{M} = \begin{pmatrix} -1 & a_1 & 0 & 0 \\ -b_1 & -1 & -c_1 & 0 \\ 0 & 0 & -1 & a_2 \\ -c_2 & 0 & -b_2 & -1 \end{pmatrix},$$

$$\mathbf{k} = \begin{pmatrix} 2g_1\big(A_{11}\,e_1^0 f_1 + A_{12}\,e_2^0 f_2\big) \\ -e_1^0\big(A_{11}\big(3f_1^2+g_1^2\big)+A_{12}\big(f_2^2+g_2^2\big)\big) - 2A_{12}\,e_2^0 f_1 f_2 \\ 2g_2\big(A_{22}\,e_2^0 f_2 + A_{21}\,e_1^0 f_1\big) \\ -e_2^0\big(A_{22}\big(3f_2^2+g_2^2\big)+A_{21}\big(f_1^2+g_1^2\big)\big) - 2A_{21}\,e_1^0 f_1 f_2 \end{pmatrix},$$

$$\mathbf{l} = \begin{pmatrix} g_1\big(A_{11}(f_1^2+g_1^2)+A_{12}\big(f_2^2+g_2^2\big)\big) \\ -f_1\big(A_{11}\big(f_1^2+g_1^2\big)+A_{12}\big(f_2^2+g_2^2\big)\big) \\ g_2\big(A_{21}\big(f_1^2+g_1^2\big)+A_{22}\big(f_2^2+g_2^2\big)\big) \\ -f_2\big(A_{21}\big(f_1^2+g_1^2\big)+A_{22}\big(f_2^2+g_2^2\big)\big) \end{pmatrix}, \tag{25}$$

where $\varepsilon_i = \epsilon_i/2 - a_i\phi_i$, $\zeta_i = a_i\epsilon_i/2 + \phi_i$, $b_i = a_i + 2A_{ii}p_i^0$, $c_1 = 2A_{12}e_1^0e_2^0$, and $c_2 = 2A_{21}e_1^0e_2^0$. The condition for one of the eigenvalues of $\mathbf{M}$ to vanish, which is a requirement for a critical point as it enables the divergent responsivity and slow critical dynamics, is that $\det\mathbf{M} = 0$, or [8]

$$(1+a_1b_1)(1+a_2b_2) = a_1a_2c_1c_2. \tag{26}$$

As the solution space is now four-dimensional, parametrized, e.g., by $(p_1^0, p_2^0, \Delta_1^0, \Delta_2^0)$, as opposed to the two-dimensional symmetric space parametrized by (p, Δ), and the space of critical points is now two- rather than one-dimensional [for example, given any (p_1^0, p_2^0) within some region, there are one or more discrete points (Δ_1^0, Δ_2^0) that are critical points], this single condition is not sufficient for a given solution to be a critical point. Rather, it describes a more general three-dimensional space that we shall call the boundary of the unstable region. The intersection of this with the two-dimensional subspace $\tilde{p}_1 = \tilde{p}_2 = 1.75$ (for $A_{11} = A_{22} = 1$, $A_{12} = A_{21} = 2$ as in Sec. II) is shown as a thick black line in Fig. 3. In fact Eq. (26) also encompasses the boundary of the other unstable region that is a generalization of the points B_1 and B_2; the symmetry-breaking-related one may be specified by $a_{1,2} > 0$, i.e., both pumps being blue-detuned from their respective Kerr-shifted resonances. We assume for the remainder of this section that Eq. (26) and $a_{1,2} > 0$ hold. The next question is how to identify which points on the edge of the unstable region are critical points. To answer this, we proceed in the same way as in Sec. II. Defining the quantities

$$Q = \frac{1+a_1b_1}{a_1c_2}, \quad R = \frac{1+a_2b_2}{1+a_1b_1},$$
$$S = \sqrt{1+a_1b_1+a_2b_2}, \tag{27}$$

and noting that (26) implies that

$$Q^2R = \frac{A_{12}\,a_2}{A_{21}\,a_1}, \tag{28}$$

the eigenvectors and eigenvalues of $\mathbf{M}$ on the boundary of the unstable region may be written as

$$\mathbf{v}_1 = \begin{pmatrix} -QRa_1 \\ -QR \\ a_2 \\ 1 \end{pmatrix}, \quad \lambda_1 = 0; \quad \mathbf{v}_2 = \begin{pmatrix} QRa_1 \\ -QR \\ -a_2 \\ 1 \end{pmatrix}, \quad \lambda_2 = -2;$$

$$\mathbf{v}_3 = \begin{pmatrix} -ia_1Q/S \\ Q \\ -ia_2/S \\ 1 \end{pmatrix}, \quad \lambda_3 = -1 + iS;$$

$$\mathbf{v}_4 = \begin{pmatrix} ia_1Q/S \\ Q \\ ia_2/S \\ 1 \end{pmatrix}, \quad \lambda_4 = -1 - iS. \tag{29}$$

The normalization of the eigenvectors is chosen to be consistent with Eq. (9) in the symmetric case. Using these new eigenvalues and eigenvectors and the corresponding inverse basis $\{\mathbf{u}_i\} : \mathbf{u}_i \cdot \mathbf{v}_j = \delta_{ij}$, where again δ_{ij} is the Kronecker delta, the reasoning in Sec. II can be replicated with just two slight modifications. Firstly, whereas in Sec. II we have $K_{111} = 0$ by symmetry, here that condition specifies the critical points. In other words, it distinguishes the critical points from the rest of the boundary of the unstable region since it implies that, in the absence of external perturbations, $\dot{\mu}_1$ is proportional to $-\mu_1^3$ rather than μ_1^2 to leading order. This is a necessary condition for a critical point since a nonzero μ_1^2 term in $\dot{\mu}_1$ would mean that μ_1 is unstable for one sign of perturbation, somewhat like a particle in an x^3 potential. This occurs everywhere on the boundary of the unstable region except for the critical point, where the stability is analogous to a particle in an x^4 potential. Conveniently, $K_{112} = -K_{111}$ on the boundary of the unstable region, so $K_{111} = 0$ implies $K_{112} = 0$, another result of directional symmetry that was used in Sec. II. The condition $K_{111} = 0$ can be expressed as

$$\big(1-3a_2^2\big)\big(QA_{22}e_2^0 - A_{12}e_1^0\big) + Q^2R^2\big(1-3a_1^2\big)\big(QA_{21}e_2^0 - A_{11}e_1^0\big) = 0. \tag{30}$$

The second slight change from Sec. II is in the resolution of the external perturbations into common- and differential-

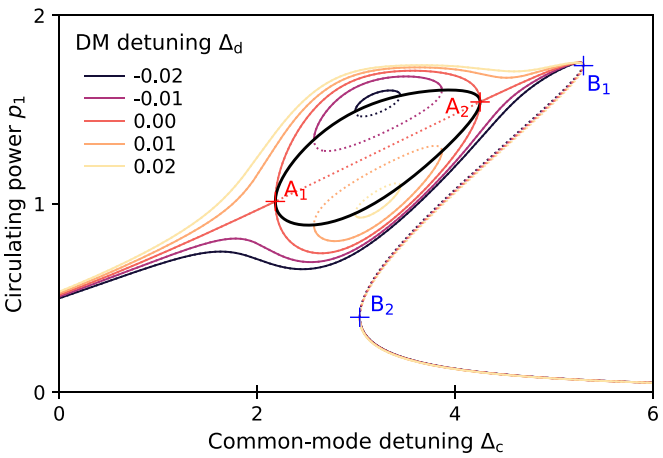

FIG. 3. Solutions to Eq. (1) under symmetric pump powers $\tilde{p}_{1,2} = \tilde{p} = 1.75$ as in Fig. 1 but for five values of the differential-mode detuning $\Delta_d = (\Delta_1 - \Delta_2)/2$, plotted as circulating power p_1 vs common-mode detuning $\Delta_c = (\Delta_1 + \Delta_2)/2$. The case $\Delta_d = 0$ and points A_1, A_2, B_1, and B_2 are as in Fig. 1, and dotted lines represent unstable solutions. The locus of the edge of the symmetry-breaking-related unstable region for varying Δ_d is shown as a thick black line.

mode components. In the general asymmetric case, the ratios of the coefficients of $\delta_{1,2}$ and $\epsilon_{1,2}$ are different in every relevant d_i or D_{ij} term. However, it is still true that d_1 must scale as μ_1^3 and $d_{3,4}$ and D_{11} as μ_1^2 in order to preserve the natural hierarchy of scalings of terms in the eigenbasis, and that no other elements of d_i or D_{ij} contribute to leading order. Therefore we may define linear combinations $\delta_{c'}$ and $\delta_{d'}$ of $\delta_{1,2}$ that scale as μ_1^2 and μ_1^3 respectively, requiring only that $\partial d_1/\partial\delta_{c'} = 0$ (and $\partial d_{3,4}/\partial\delta_{c'}$, $\partial D_{11}/\partial\delta_{c'} \neq 0$), and still satisfy the scalings of d_1, $d_{3,4}$, and D_{11} to leading order. Since

$$d_1 = \frac{Qe_2^0\delta_2 - e_1^0\delta_1}{2Q(1+R)} + \frac{Qa_1(1+a_2^2)e_2^0\epsilon_2 - a_2(1+a_1^2)e_1^0\epsilon_1}{4a_1a_2Q(1+R)} \tag{31}$$

we shall do this as follows:

$$\delta_{c'} = \frac{1}{2}\left(\delta_1 + \frac{Qe_2^0}{e_1^0}\delta_2\right), \quad \delta_{d'} = \frac{1}{2}\left(\delta_1 - \frac{Qe_2^0}{e_1^0}\delta_2\right). \tag{32}$$

Similarly, for $\epsilon_{1,2}$ we define

$$\epsilon_{c'} = \frac{1}{2}\left(\epsilon_1 + \frac{Qa_1(1+a_2^2)e_2^0}{a_2(1+a_1^2)e_1^0}\epsilon_2\right),$$
$$\epsilon_{d'} = \frac{1}{2}\left(\epsilon_1 - \frac{Qa_1(1+a_2^2)e_2^0}{a_2(1+a_1^2)e_1^0}\epsilon_2\right), \tag{33}$$

so that $\partial d_1/\partial\epsilon_{c'} = 0$. Finally, as in Sec. II, we can express the dynamics of μ_1 in the form

$$\dot{\mu}_1 = d_1 + D_{11}^{\text{eff}}\,\mu_1 + L_{1111}^{\text{eff}}\,\mu_1^3, \tag{34}$$

where

$$D_{11}^{\text{eff}} = D_{11} - 2\left(\frac{K_{113}d_3}{\lambda_3} + \frac{K_{114}d_4}{\lambda_4}\right) \quad \text{and}$$
$$L_{1111}^{\text{eff}} = L_{1111} - 2\left(\frac{K_{113}K_{311}}{\lambda_3} + \frac{K_{114}K_{411}}{\lambda_4}\right), \tag{35}$$

applying the transformation

$$x = D_{11}^{\text{eff}}, \quad y = -\sqrt{-L_{1111}^{\text{eff}}}\,\mu_1, \quad z = -\sqrt{-L_{1111}^{\text{eff}}}\,d_1 \tag{36}$$

to reproduce Eq. (20), which works because $L_{1111}^{\text{eff}} < 0$. The quantities d_1, D_{11}^{eff} (to leading order) and L_{1111}^{eff} [simplified a little by assuming Eq. (30)] are given by

$$d_1 = -\frac{e_1^0(2a_1\delta_{d'} + (1+a_1^2)\epsilon_{d'})}{2Q(1+R)a_1}, \tag{37}$$

$$D_{11}^{\text{eff}} = \frac{1}{2a_1^2a_2Q^2(1+R)}\Bigg(\frac{a_1Q(a_1(a_2^2-1)e_1^0 + (a_1^2-1)a_2e_2^0QR)\delta_{c'}}{e_2^0}$$
$$+ \frac{e_1^0}{1+S^2}\big(a_1\{Q[a_2(1-3a_2^2)A_{22}e_2^0 + a_1(1-a_2^2)A_{21}e_1^0Q] + 2A_{12}a_2^2(a_2e_1^0 + a_1e_2^0Q)\}$$
$$+ a_2Q[(1-a_1^2)A_{12}a_2e_2^0 + a_1(1-3a_1^2)A_{11}e_1^0Q]R)[2a_1\delta_{c'} + (1+a_1^2)\epsilon_{c'}]\Bigg), \tag{38}$$

$$L_{1111}^{\text{eff}} = \frac{1}{2a_1^2a_2(1+R)}\Bigg(a_1[a_1(1-a_2^4)A_{22} + 2A_{12}a_2(1-a_1^2a_2^2)R + (1-a_1^4)A_{11}a_2Q^2R^3]$$
$$- \frac{2}{Q^2(1+S^2)}[2a_1A_{12}(1-a_2^2)e_1^0 - a_1(1-3a_2^2)A_{22}e_2^0Q + (1+a_1^2)A_{12}a_2e_2^0QR]$$
$$(a_1\{Q[a_2(1-3a_2^2)A_{22}e_2^0 + a_1(1-a_2^2)A_{21}e_1^0Q] + 2A_{12}a_2^2(a_2e_1^0 + a_1e_2^0Q)\}$$
$$+ a_2Q[(1-a_1^2)A_{12}a_2e_2^0 + a_1(1-3a_1^2)A_{11}e_1^0Q]R)\Bigg). \tag{39}$$

The deviations $\delta p_{1,2}$ of the circulating powers $p_{1,2}$ from their steady-state values $p_{1,2}^0$ are given to leading order by $2e_i^0 f_i$, or

$$\delta p_1 = -2QRa_1e_1^0\mu_1, \quad \delta p_2 = 2a_2e_2^0\mu_1. \tag{40}$$

As a final comment, it is worth noting that microresonators generally possess strong thermal nonlinearity due to a combination of thermorefractive effects and thermal expansion [35]. This typically creates circulating-power-dependent resonance frequency shifts between one and two orders of magnitude larger than the Kerr shifts, but which require much longer timescales to take effect, and could thus greatly complicate the critical dynamics. Importantly, however, these effects depend only on the total circulating power $p_1 + p_2$ and create equal shifts for both directions, i.e., change Δ_1 and Δ_2, or equivalently δ_1 and δ_2, by the same amount, assuming that the two modes occupy the exact same region. This means that they can be decoupled from the critical dynamics in two ways: firstly by making δp_1 and δp_2 in Eq. (40) equal and opposite, and secondly by making the coefficients of δ_1 and δ_2 in $\delta_{d'}$ [Eq. (32)] equal and opposite. The latter condition may be written as

$$Qe_2^0 = e_1^0, \tag{41}$$

while the former simplifies via Eq. (28) to

$$QA_{21}e_2^0 = A_{12}e_1^0. \tag{42}$$

Thus the two conditions are equivalent if $A_{21} = A_{12}$, which is in fact necessarily true due to the reciprocity of the Kerr effect, since the normalization factor for the circulating power is the same for both modes.

IV. CONCLUSION AND OUTLOOK

We have derived a theory that explains the dynamics of a bidirectionally pumped optical resonator with Kerr nonlinearity in the region close to the critical point of the symmetry breaking between counterpropagating light. The response of the system to both pump detuning and pump power perturbations is examined, and it is shown that a given fractional pump power perturbation has a very similar effect to a pump detuning perturbation that is roughly the same fraction of the resonator's linewidth. The analysis was done first for the case of a perfectly symmetrical system in Sec. II, before being generalized to asymmetrical pumping conditions and SPM and XPM coefficients in Sec. III. A condition for compensating the various asymmetries with each other to recover a critical point is derived [Eqs. (26) and (30)]. The critical dynamics are shown to be described by the simple Eq. (20) in both the symmetric and asymmetric cases, for each of which explicit formulas for the conversion factors to the generalized variables x, y, and z are obtained. From Eq. (20), we see that the system exhibits scaling invariance, divergent steady-state responsivity and critical slowing down, all of which are universal features of critical systems. Finally, a condition for decoupling the critical dynamics from thermal nonlinearities is discussed.

The theory presented here describes in detail the response of critical-point-enhanced sensors such as gyroscopes [14,15] and refractive index sensors [18]. Furthermore, it is applicable to any optical resonator in which two modes interact via the Kerr nonlinearity, including modes of different frequencies, propagation angles [27] or opposite circular polarizations [26,28–30]. It also extends to other Kerr-like effects such as the magnetic nonlinearity [33], and even to similar nonlinear systems outside the optical domain.

ACKNOWLEDGMENTS

The authors would like to thank Lewis Hill, Michael Woodley, and Leonardo Del Bino for helpful discussions. This work was supported by the Royal Academy of Engineering and the Office of the Chief Science Adviser for National Security under the UK Intelligence Community Postdoctoral Fellowship Programme. The authors also acknowledge funding from H2020 Marie Sklodowska-Curie Actions (MSCA) (No. 748519, CoLiDR), H2020 European Research Council (ERC) (No. 756966, CounterLight), and National Physical Laboratory Strategic Research.

[1] P. W. Higgs, Broken Symmetries and the Masses of Gauge Bosons, Phys. Rev. Lett. **13**, 508 (1964).
[2] J. Bardeen, L. N. Cooper, and J. R. Schrieffer, Theory of superconductivity, Phys. Rev. **108**, 1175 (1957).
[3] L. Landau, Theory of the superfluidity of helium II, Phys. Rev. **60**, 356 (1941).
[4] I. Bloch, J. Dalibard, and W. Zwerger, Many-body physics with ultracold gases, Rev. Mod. Phys. **80**, 885 (2008).
[5] H. E. Stanley, *Phase Transitions and Critical Phenomena* (Clarendon Press, Oxford, 1971).
[6] L. Del Bino, J. M. Silver, S. L. Stebbings, and P. Del'Haye, Symmetry breaking of counter-propagating light in a nonlinear resonator, Sci. Rep. **7**, 43142 (2017).
[7] Q. T. Cao, H. M. Wang, C. H. Dong, H. Jing, R. S. Liu, X. Chen, L. Ge, Q. H. Gong, and Y. F. Xiao, Experimental Demonstration of Spontaneous Chirality in a Nonlinear Microresonator, Phys. Rev. Lett. **118**, 033901 (2017).
[8] M. T. M. Woodley, J. M. Silver, L. Hill, F. Copie, L. Del Bino, S. Y. Zhang, G. L. Oppo, and P. Del'Haye, Universal symmetry-breaking dynamics for the Kerr interaction of counterpropagating light in dielectric ring resonators, Phys. Rev. A **98**, 053863 (2018).
[9] L. Del Bino, J. M. Silver, M. T. M. Woodley, S. L. Stebbings, X. Zhao, and P. Del'Haye, Microresonator isolators and circulators based on the intrinsic nonreciprocity of the Kerr effect, Optica **5**, 279 (2018).
[10] N. Moroney, L. Del Bino, M. T. M. Woodley, G. N. Ghalanos, J. M. Silver, A. O. Svela, S. Zhang, and P. Del'Haye, Logic gates based on interaction of counterpropagating light in microresonators, J. Lightwave Technol. **38**, 1414 (2020).
[11] L. Del Bino, N. Moroney, and P. Del'Haye, Optical memories and switching dynamics of counterpropagating light states in microresonators, Opt. Express **29**, 2193 (2021).
[12] M. T. M. Woodley, L. Hill, L. Del Bino, G.-L. Oppo, and P. Del'Haye, Self-Switching Kerr Oscillations of Counterpropagating Light in Microresonators, Phys. Rev. Lett. **126**, 043901 (2021).
[13] E. J. Post, Sagnac effect, Rev. Mod. Phys. **39**, 475 (1967).
[14] A. E. Kaplan and P. Meystre, Enhancement of the Sagnac effect due to nonlinearly induced nonreciprocity, Opt. Lett. **6**, 590 (1981).
[15] C. Wang and C. P. Search, Enhanced rotation sensing by nonlinear interactions in silicon microresonators, Opt. Lett. **39**, 4376 (2014).
[16] J. M. Silver, L. Del Bino, M. T. M. Woodley, G. N. Ghalanos, A. Ø. Svela, N. Moroney, S. Zhang, K. T. V. Grattan, and P. Del'Haye, Nonlinear enhanced microresonator gyroscope, Optica **8**, 1219 (2021).
[17] S. Maayani, R. Dahan, Y. Kligerman, E. Moses, A. U. Hassan, H. Jing, F. Nori, D. N. Christodoulides, and T. Carmon, Flying couplers above spinning resonators generate irreversible refraction, Nature (London) **558**, 569 (2018).
[18] C. Wang and C. P. Search, A nonlinear microresonator refractive index sensor, J. Lightwave Technol. **33**, 4360 (2015).
[19] A. Ø. Svela, J. M. Silver, L. Del Bino, G. Ghalanos, N. Moroney, M. T. Woodley, S. Zhang, M. Vanner, and

P. Del'Haye, Spontaneous symmetry breaking based near-field sensing with a microresonator, in *CLEO: QELS_Fundamental Science* (Optical Society of America, Washington, DC, 2019), p. JM3B–3.

[20] Y.-H. Lai, Y.-K. Lu, M.-G. Suh, Z. Yuan, and K. Vahala, Observation of the exceptional-point-enhanced Sagnac effect, Nature (London) **576**, 65 (2019).

[21] M. P. Hokmabadi, A. Schumer, D. N. Christodoulides, and M. Khajavikhan, Non-Hermitian ring laser gyroscopes with enhanced Sagnac sensitivity, Nature (London) **576**, 70 (2019).

[22] W. Langbein, No exceptional precision of exceptional-point sensors, Phys. Rev. A **98**, 023805 (2018).

[23] H.-K. Lau and A. A. Clerk, Fundamental limits and non-reciprocal approaches in non-Hermitian quantum sensing, Nat. Commun. **9**, 4320 (2018).

[24] H. Wang, Y.-H. Lai, Z. Yuan, M.-G. Suh, and K. Vahala, Petermann-factor sensitivity limit near an exceptional point in a Brillouin ring laser gyroscope, Nat. Commun. **11**, 1610 (2020).

[25] R. W. Boyd, *Nonlinear Optics* (Academic Press, New York, 1992).

[26] B. Garbin, J. Fatome, G.-L. Oppo, M. Erkintalo, S. G. Murdoch, and S. Coen, Asymmetric balance in symmetry breaking, Phys. Rev. Res. **2**, 023244 (2020).

[27] M. Haelterman, All-optical set-reset flip-flop operation in the nonlinear Fabry-Perot interferometer, Opt. Commun. **86**, 189 (1991).

[28] I. Areshev, T. Murina, N. Rosanov, and V. Subashiev, Polarization and amplitude optical multistability in a nonlinear ring cavity, Opt. Commun. **47**, 414 (1983).

[29] M. Haelterman, S. Trillo, and S. Wabnitz, Polarization multistability and instability in a nonlinear dispersive ring cavity, J. Opt. Soc. Am. B **11**, 446 (1994).

[30] F. Copie, M. T. M. Woodley, L. Del Bino, J. M. Silver, S. Y. Zhang, and P. Del'Haye, Interplay of Polarization and Time-Reversal Symmetry Breaking in Synchronously Pumped Ring Resonators, Phys. Rev. Lett. **122**, 013905 (2019).

[31] J. Fatome, J. Fatome, J. Fatome, B. Kibler, F. Leo, A. Bendahmane, G.-L. Oppo, B. Garbin, B. Garbin, B. Garbin, S. G. Murdoch, S. G. Murdoch, M. Erkintalo, M. Erkintalo, S. Coen, and S. Coen, Polarization modulation instability in a nonlinear fiber Kerr resonator, Opt. Lett. **45**, 5069 (2020).

[32] B. Garbin, J. Fatome, G.-L. Oppo, M. Erkintalo, S. G. Murdoch, and S. Coen, Dissipative Polarization Domain Walls in a Passive Coherently Driven Kerr Resonator, Phys. Rev. Lett. **126**, 023904 (2021).

[33] D. A. Martin and M. Hoyuelos, Homogeneous solutions for elliptically polarized light in a cavity containing materials with electric and magnetic nonlinearities, Phys. Rev. A **82**, 033841 (2010).

[34] L. Hill, G.-L. Oppo, M. T. M. Woodley, and P. Del'Haye, Effects of self- and cross-phase modulation on the spontaneous symmetry breaking of light in ring resonators, Phys. Rev. A **101**, 013823 (2020).

[35] T. Carmon, L. Yang, and K. J. Vahala, Dynamical thermal behavior and thermal self-stability of microcavities, Opt. Express **12**, 4742 (2004).

[36] J. M. Silver and P. Del'Haye, Generalized theory of optical resonator and waveguide modes and their linear and Kerr nonlinear coupling, arXiv:2103.10479.